Available online at www.sciencedirect.com
ScienceDirect
Aerosol Science 38 (2007) 719–727
Journal of Aerosol Science
www.elsevier.com/locate/jaerosci

Penetration of 4.5 nm to 10 μm aerosol particles through fibrous filters

Sheng-Hsiu Huang[a], Chun-Wan Chen[a], Cheng-Ping Chang[a], Chane-Yu Lai[b], Chih-Chieh Chen[c,*]

[a]*Institute of Occupational Safety and Health, Council of Labor Affairs, No. 99, Lane 407, Heng-Ke Road, Shijr City, Taipei, Taiwan*
[b]*Department of Occupational Safety & Health, College of Health Care & Management, Chung Shan Medical University, No. 110, Section 1, Chien-Kuo North Rd., Room 511, Taichung 402, Taiwan*
[c]*Institute of Occupational Medicine and Industrial Hygiene, College of Public Health, National Taiwan University, 17 Xu-Zhou Road, Room 718, Taipei, Taiwan*

Received 4 April 2006; received in revised form 25 May 2007; accepted 25 May 2007

Abstract

This study presents the experimental results of penetration of aerosol particles with diameters between 4.5 nm and 10 μm through fibrous filters. Three particle size spectrometers: the TSI 3080 electrostatic classifier equipped with nano- or long differential mobility analyzer, and the TSI 3321 aerodynamic particle sizer, were used to measure nanometer, submicron, and micron-sized particles. NaCl aerosol particles were generated by using spray-drying methods. To eliminate electrostatic charges, filters were dipped in isopropanol for 5 min and allowed to dry. These dipped filters, along with controls of each filter type, were then tested to determine the aerosol penetrations in the size range of 4.5 nm–10 μm. The experimental results demonstrated that almost all particles with sizes below 10 nm or exceeding 5 μm were collected in the filters, and the filter charge density did not significantly affect the penetration values. The results also suggested that there is no thermal rebound of particles in the size range down to 4.5 nm in fibrous filters.

Keywords: Thermal rebound; Nanoparticle; Aerosol spectrometer; Filtration mechanism

1. Introduction

Currently, nanotechnology is increasingly being used to produce new and improved products. Consequently, the numbers of workers exposed to nanoparticles may increase markedly in the near future. Nanoparticles differ from larger particles in deposition behavior and alveolar clearance efficiency. Epidemiological studies indicate that exposure to nanoparticles may cause pulmonary diseases, cardiovascular health effects and immune system impairment (Dockery & Pope, 1994; Hagdnagy, Stiller-Winkler, Kainka, Ranft, & Idel, 1998). Although the epidemiology does not make it clear whether the mass, number or even surface area of particles is the most important determinant of health impact, some toxicological studies demonstrate that nanoparticles exert a much stronger physiological effect than an equivalent mass of coarse particles (Donaldson, Li, & Mac-Nee, 1998; Oberdorster, Ferin, Gelein, Soderholm, & Finkelstein,

* Corresponding author. Tel.: +886 2 33228086; fax: +886 2 23938631.
E-mail address: ccchen@ntu.edu.tw (C.-C. Chen).

0021-8502/$ - see front matter © 2007 Elsevier Ltd. All rights reserved.
doi:10.1016/j.jaerosci.2007.05.007

1992). Therefore, the toxicological mechanisms behind these effects and the concentrations of ambient particulate matter should be accounted for by the nanoparticle fraction, which has a negligible mass concentration.

Particulate respirators are widely used in workplaces to protect against hazardous airborne particles. Filtering facepieces are the most popular form of respirator among workers because of their lightness, better vision, and low maintenance compared with elastometric respirators (Chen & Huang, 1998). The performance of filter media has been extensively tested using non-biological particles (Chen & Huang, 1998; Chen & Willeke, 1992; Chen, Lehtimaki, & Willeke, 1992; Martin & Moyer, 2000) and biological particles (McCullough, Brosseau, & Vesley, 1997; Qian, Willeke, Grinshpun, Donnelly, & Coffey, 1998; Willeke, Qian, Donnelly, Grinshpun, & Ulevicius, 1996). However, most of these studies focused on particle sizes above 100 nm. Because of increasing concern regarding the health effects associated with the production of nanomaterials and other nanoparticle related issues, an urgent need exists for performance assessment for filter media in the nano-sized range.

Concerning the penetration of nano-sized aerosol particles through filter media, the only experimental data available to date are those of Balazy, Podgorsky, and Gradon (2004). In this study, they used the aerosol spectrometer that combines the principles of differential mobility analysis (DMA) and condensation particle counting (CPC) to measure the particle sizes and number concentrations. The experimental results showed that particles with diameter $\leqslant 20$ nm had penetrations exceeding those predicted by the classical theory of depth filtration. Balazy et al. (2004) used the thermal rebound theory to explain the higher penetration values. Moreover, Wang and Kasper (1991) developed a model, which incorporates the effect of particle rebound from the filter surface due to thermal velocity, to predict the filtration efficiency of nanoparticles. They found that the thermal impact velocity exceeds the critical sticking velocity in the particle size between 1 and 10 nm. Consequently, the classical trend of the efficiency curve for particle size below 10 nm is reversed.

However, it was shown that the aerosol spectrometer combining the principles of DMA and CPC, can cause error when given a high scan speed (TSI, 2002). In this case, a small tail might appear on the left side of the displayed distribution. However, the particles displayed on the nanometer-sized range are not real. It is likely due to the residual particles counted by the CPC from the previous down scan, as will be discussed below. Consequently, the accuracy of filtration efficiencies calculated based on these data is questionable. Therefore, the main objective of the present study was to investigate the filtration characteristics of nanoparticles penetrating through commercialized filtering facepieces. Moreover, the penetration values of submicrometer- and micrometer-sized particles were also presented.

2. Experimental materials and methods

Fig. 1 schematically shows the test system for measuring the particle penetration through filter media. To determine the particle penetration as a function of particle size in the range of 4.5–10 μm, three aerosol generation systems were used to produce particles with different size distributions. The test material was sodium chloride (NaCl). A constant output atomizer (model 3076, TSI Inc., St. Paul, MN) and an ultrasonic atomizing nozzle (model 8700-120, Sonotek Inc., Highland, NY) were used to generate polydisperse submicrometer-sized and micrometer-sized challenge aerosol particles, respectively. Additionally, a homemade atomizer was operated with a very dilute NaCl solution to produce nano-sized aerosol particles. Table 1 listed the size distribution characteristics of challenge aerosol particles used in this work. In order to exclude the electrostatic effects, the generated particles were then passed through an aerosol neutralizer (25 mCi, Am 241) to neutralize the aerosol particles to the Boltzmann charge equilibrium. Next, the neutralized aerosols were mixed with dried and filtered air to obtain the desired flow rates. The aerosol particles were completely dried before entering the filter test system. In this work, the air flow rate was 85 L/min, unless otherwise specified.

Two particle size spectrometers, a scanning mobility particle sizer (SMPS, model 3936, TSI Inc.) and an aerodynamic particle sizer (APS, model 3321, TSI Inc.) were used to measure the aerosol concentrations and size distributions. The SMPS spectrometer measures the size distribution of submicrometer aerosols using an electrical mobility detection technique. The particles are classified using an electrostatic classifier (model 3080, TSI Inc.) with a long-DMA (model 3081, TSI Inc.) or a nano-DMA (model 3085, TSI Inc.) for particles in the size ranges 14–750 nm and 5–165 nm, respectively. The particle concentrations are measured using a CPC (model 3022A, TSI Inc.). The APS, which uses the time-of-flight particle sizing technology, could count and size particles ranging from 0.5–20 μm. Both particle size spectrometers were calibrated using the polystyrene latex, PSL, particles (Duke Scientific Corp.). Particle number concentration data, obtained upstream and downstream of the filter media, respectively, were used to assess the penetration of aerosol particles.

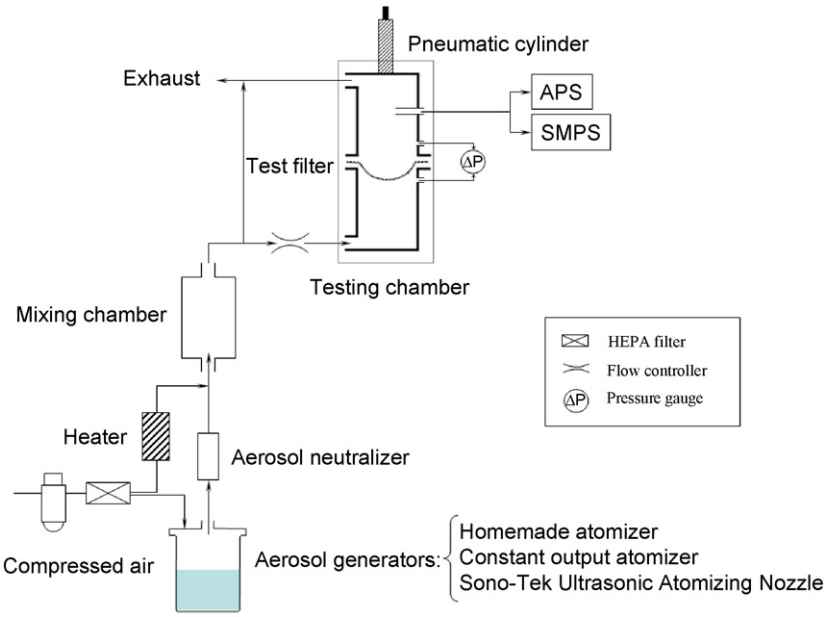

Fig. 1. Schematic diagram of the experimental set-up.

Table 1
The size distribution characteristics of challenge aerosol particles

Aerosol generator	Particle size distribution		
	Count median diameter (nm)	Geometric standard deviation	Number concentration (#/cm^3)
Homemade atomizer	9	1.50	1.3×10^4
Constant output atomizer	78	1.86	1.0×10^6
Sono-Tek ultrasonic atomizing nozzle	1300	1.30	478

Two commercially available filtering facepiece respirators (hereafter referred to as A and B), were chosen for this study. Respirator A equips with an NIOSH approved N95 class filter, and respirator B has a FFP1 (EN149:2001) mask. The filters were tested as received and no temperature and relative humidity pretreatment was performed before testing. However, to study the impact of electrostatic charges on collection efficiency, filters were dipped in isopropanol for 5 min and dried naturally. Previous studies have shown that this process removes the electrical charge associated with the filter fibers (Chen & Huang, 1998; Chen, Lehtimaki, & Willeke, 1993; Martin & Moyer, 2000). These dipped filters, along with controls of each filter type, were then tested to determine the initial aerosol penetration for particles in the size ranging from 4.5 nm to 10 μm.

As showed in Fig. 1, the testing chamber that had an internal diameter of 10.8 cm was comprised of two metal cups with special gaskets which seal around the filter media. A non-rotating air cylinder was used to compress the filter media between the caps. The aerosol penetration tests were performed by operating the testing chamber without and with a filter to obtain upstream and downstream particle concentrations, respectively. Therefore, the error due to particle losses was eliminated because of the identical sampling line. Moreover, the CPC induced measurement artifacts that presented in Heim, Mullins, Wild, Meyer, and Kasper (2005) were also eliminated because only one SMPS was used to measure the upstream and downstream particle concentrations.

Besides the experimental penetrations, the theoretical predictions based on the classic single fiber theory of depth filtration, which was used in the previous study (Chen & Huang, 1998) were also presented for comparison with the experimental data. The theoretical aerosol penetration of a particle with n elementary charges, P_n, through a filter is

normally expressed in terms of total single fiber efficiency, $E_{\Sigma,n}$ (Hinds, 1999)

$$P_n = \exp\left[\frac{-4\alpha x E_{\Sigma,n}}{\pi d_f(1-\alpha)}\right],$$

where α is packing density, χ is filter thickness, d_f is fiber diameter, and $E_{\Sigma,n}$ is given by (Lathrache & Fissan, 1987; Tennal, Mazumder, Siag, & Reddy, 1991)

$$E_{\Sigma,n} = 1 - (1 - E_m)(1 - E_{e,n}).$$

In Eq. (3), E_m is the total single fiber efficiency due to the mechanical force, given as

$$E_m = 1 - (1 - E_{dr})(1 - E_i)(1 - E_g)$$

and $E_{e,n}$ is the total single fiber efficiency due to the electrical force, given as

$$E_{e,n} = 1 - (1 - E_p)(1 - E_{c,n})(1 - E_{m,n}),$$

where E_{dr} is due to diffusion and interception (Lee & Liu, 1982); E_i is due to impaction (Hinds, 1999); E_g is due to gravitational settling (Hinds, 1999); E_p is due to dielectrophoretic force; $E_{c,n}$ is due to Coulombic force (Lathrache & Fissan, 1987; Tennal et al., 1991); and $E_{m,n}$ is due to image force (Kanaoka, Emi, Otani, & Iiyama, 1987). The above equation is an approximation based on the assumptions that the electret filters have a uniform charge on their fibers and all individual filtration mechanisms are independent. It is assumed that the particle charges are in Boltzmann charge equilibrium, and the interaction terms between the individual mechanisms are not within the scope of the present study. A spreadsheet (Microsoft Excel) was used to calculate and integrate the filtration efficiency by each individual filtration mechanism. The in-depth information of all individual filtration mechanisms has been summarized previously (Chen et al., 1993) and is not reiterated here.

3. Results and discussions

Fig. 2, which comprises the data from two particle size spectrometers, the SMPS and the APS, displays the aerosol penetration through filter A with and without the isopropanol dip. The filters with the electrostatic charge removed show a clear and significant increase in aerosol penetration, particularly for particles in the 0.1–1 μm size range, indicating that electrostatic attraction is an important mechanism for filters when collecting submicrometer-sized particles. The maximum penetrations increase from approximately 5.8% to around 18.9%. However, for particles with sizes of below

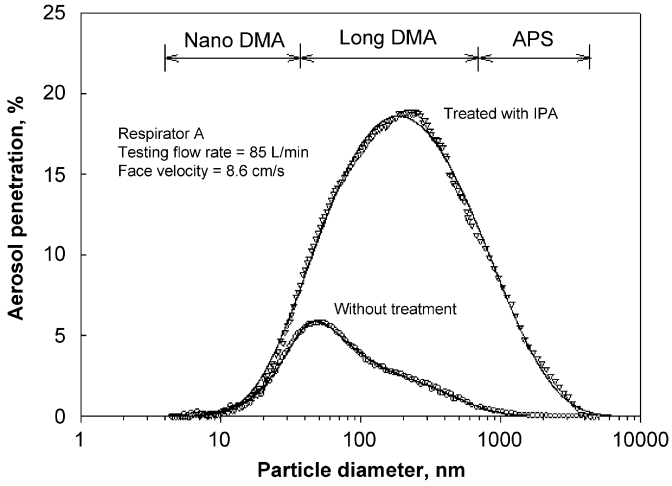

Fig. 2. Aerosol penetration through respirator A with and without isopropanol dip for a flow rate of 85 L/min (face velocity = 8.6 cm/s).

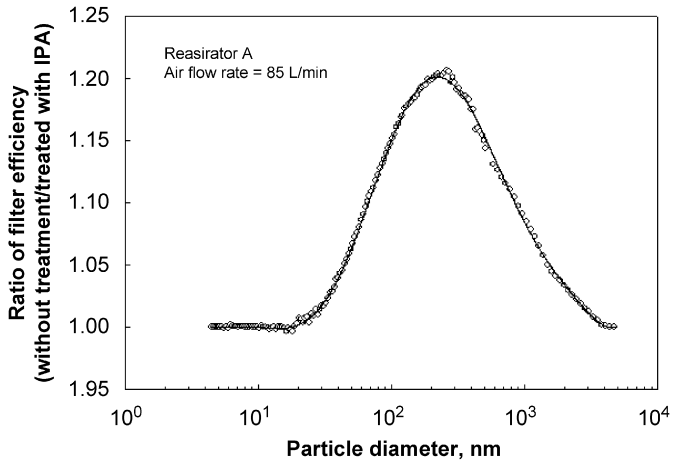

Fig. 3. Ratio of aerosol particle removal by electret versus mechanical respirator A for a flow rate of 85 L/min (face velocity = 8.6 cm/s).

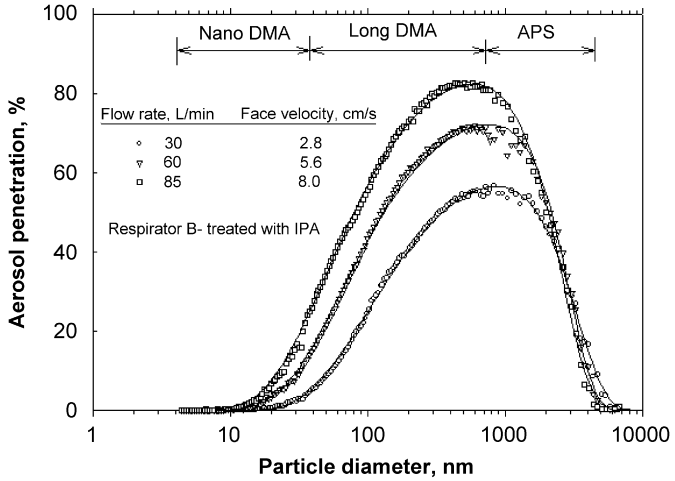

Fig. 4. Effect of testing flow rate on the aerosol penetration through treated respirator B.

10 nm and above 5 μm, the penetrations were close to zero regardless of whether or not the filters had charges, implying that electrostatic force is not a dominant filtration mechanism for the above particle size ranges. Moreover, in contrast with the conclusion of previous studies (Balazy et al., 2004; Wang & Kasper, 1991), the present experimental results indicate that thermal rebound phenomena for nanoparticle collection must be ruled out. The result on nanoparticle filtration characteristic is in line with the finding of Heim et al. (2005).

This figure also shows a clear shift in the most penetrating particle size. For electret filters, the most penetrating particle size was about 50 nm, agreeing with the result of previous studies (Balazy et al., 2006a, 2006b). However, once the electrostatic charge was removed from the filter fibers, the most penetrating particle size clearly shifted toward larger size. In this case, it was 200 nm. The effect of fiber charge on the shifting of the most penetrating particle size has also been mentioned (Chen & Huang, 1998; Balazy et al., 2006b). The filter efficiencies (100—penetration %) shown in Fig. 2 are used to calculate the ratio of aerosol particle removal by electret versus mechanical filters, as illustrated in Fig. 3. As expected, the improvement of filter efficiency by electrostatic forces is significant for submicrometer-sized particles. For this filter and testing air flow rate, the maximum efficiency ratio is approximately 1.2 at particle size of 260 nm.

The experiments with less efficient filter at different testing flow rates did not reveal any new features. Fig. 4 shows the performances of respirator B, which was treated with isopropanol, at different testing flow rates. The

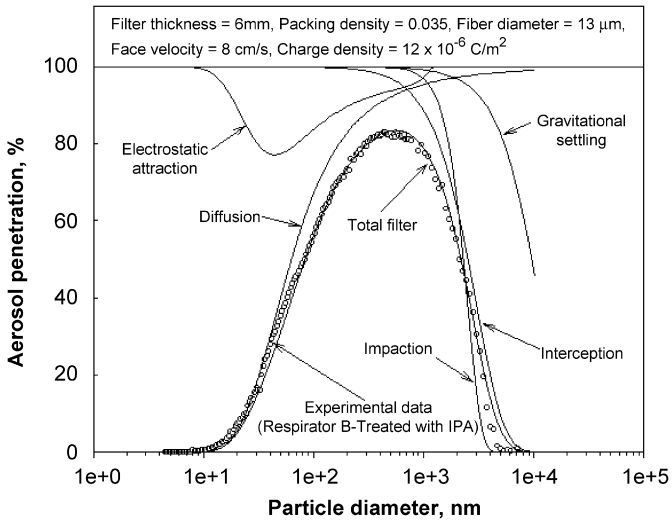

Fig. 5. Comparison of theoretical calculations to experimental data of respirator B (treated with isopropanol) for a flow rate of 85 L/min (face velocity = 8.6 cm/s).

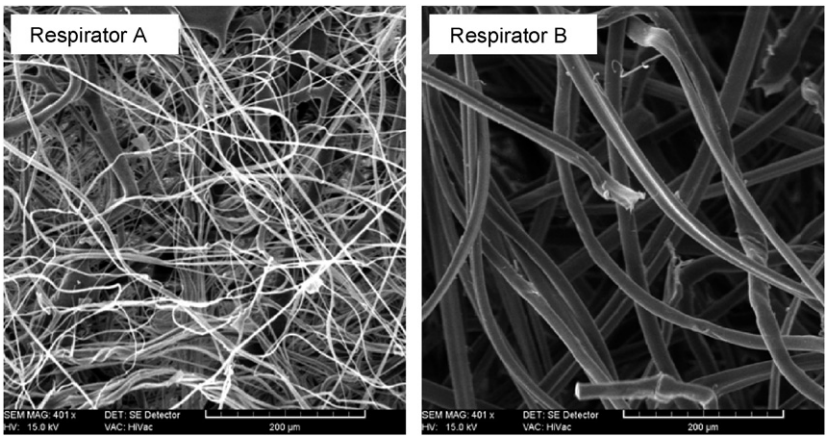

Fig. 6. Scanning electron micrographs of respirator A and B.

penetrations of submicrometer-sized particles clearly increased with testing flow rate, indicating that this respirator removed submicrometer-sized particles via diffusion. For example, the penetrations of 300 nm particles through this filter were 47%, 66%, and 79% at testing flow rates of 30, 60, and 85 L/min, respectively. Conversely, the penetrations of micrometer-sized particles through the treated filter decrease with increasing testing flow rate, indicating that this respirator removed micrometer-sized particles by impaction. This unique pattern was also observed in the previous study (Chen & Huang, 1998). For this filter, the most penetrating particle sizes were 835, 777, and 723 nm for testing flow rates of 30, 60 and 85 L/min, respectively. As aforementioned, the penetrations of particles smaller than the most penetrating particle size decreased with decreasing particle sizes owing to diffusion becoming dominant. For particles sized 10 nm and smaller, the penetrations reached almost 0%, and thermal rebound effects were not observed.

Fig. 5 compares theoretical calculations with the experimental data of the treated respirator B at a testing flow rate of 85 L/min. Respirator B was chosen because of the more uniform fiber diameter, as shown in Fig. 6. Therefore, the calculation bias due to the variability in fiber diameter was minimized. The solid line in Fig. 5, indicates the total filter efficiency and the efficiency due to each of the single fiber mechanisms; moreover, the open symbol represents the experimental data. The filter and fiber properties of the tested respirators were determined carefully in the present

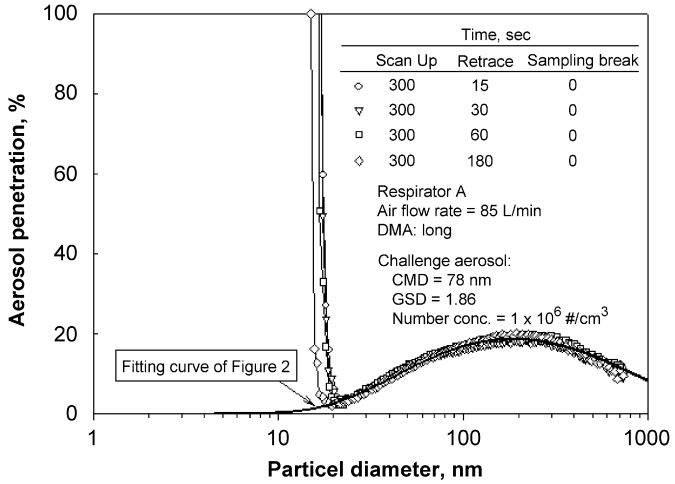

Fig. 7. Effect of retrace time on the aerosol penetration curves when using the SMPS equipped with a long-DMA as an aerosol spectrometer.

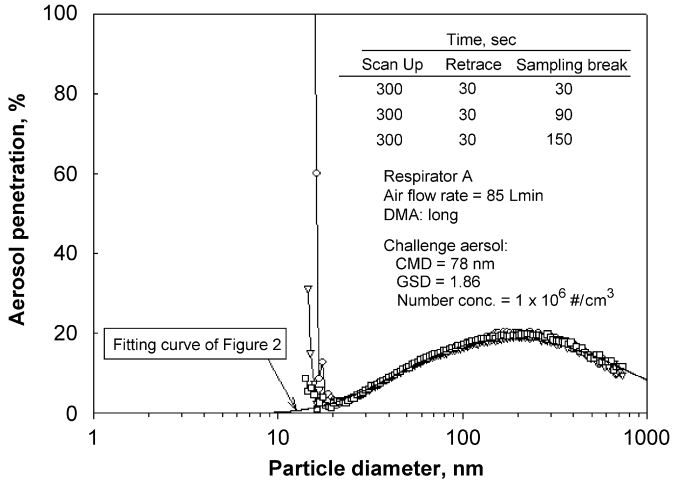

Fig. 8. Effect of sample space on the aerosol penetration curves when using the SMPS equipped with a long-DMA as an aerosol spectrometer.

study. The filter thickness was measured as 6 mm by using a vernier caliper. An equivalent fiber diameter of 13 μm was determined by back-calculating to fit the modeled data to the experimental data (Chen & Huang, 1998; Balazy et al., 2006a, 2006b). This value was in reasonable agreement with the electron micrograph images shown in Fig. 6. The packing density can be calculated based on the density of the fiber material and the weight of a known volume of filter sample. Although isopropanol appeared to reduce the electrostatic charges on the filter fibers, a small residual charge was shown to be left on the fibers (Chen & Huang, 1998; Chen et al., 1993). Accordingly, a charge density of $1.2 \times 10^{-6}\,\mathrm{C/m^2}$ also determined by back-calculating method, was used in the calculations. Using these equivalent values, a near perfect match exists between the single fiber efficiency calculation and the experimental data, as illustrated in Fig. 5. As expected, diffusion is the only important mechanism for collecting particles below 300 nm, and impaction and interception are the dominant mechanisms for collecting particles larger than 1 μm.

The SMPS program has two scan time settings, Scan Up and Scan Retrace, to provide a complete run of sample analysis. Scan Up time is the period during which the classifier center rod voltage exponentially increases in magnitude. Size distribution data is sampled during Scan Up. Meanwhile, Scan Retrace time is the period during which the classifier voltage is lowered, or retraced, to its initial voltage. For continuous sampling, the time between two runs termed

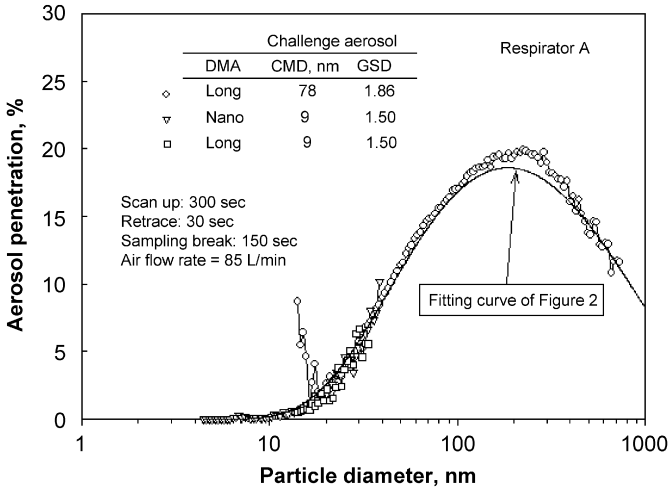

Fig. 9. Effect of size distributions of challenge aerosol on the aerosol penetration curves, measured using different model of DMA (long- and nano-DMA).

"sampling break". Figs. 7 and 8 demonstrate the order of magnitude of the error associated with using the SMPS to measure aerosol penetration through filter media. Fig. 7 shows the influence of retrace speeds on aerosol penetration curves. The solid line represents the fitting curve of aerosol penetration data of treated respirator A in Fig. 2. As shown in Fig. 7, when the sampling break was set to 0 s, the retrace speed did not affect the aerosol penetrations of particles larger than 20 nm. However, the trend of the aerosol penetration curves was reversed for particles smaller than 20 nm. The aerosol penetration increased dramatically with decreasing particle size. As mentioned previously, this phenomenon results from the artifacts in CPC counting efficiency. Although the error magnitude could be reduced by increasing the sampling break, as shown in Fig. 8, the aerosol penetrations for particles sized less than 20 nm were still overestimated.

If this data is not double checked, it may mislead to the conclusion that the experimental penetrations would be higher than the theoretically predicted ones, reaching the inference of the false possibility of having thermal rebound phenomena. The error might be greater for higher efficiency filters challenged against particles with larger count median diameter (CMD). However, challenging the filter against particles with a smaller CMD can further minimize this error, as can be seen in Fig. 9. Good agreement is obtained between the penetration data by using a long-DMA and a nano-DMA. Since the modal diameter of the challenge aerosol used in Balazy et al. (2004) was around 200 nm, only a small number of particles were in the size less than 20 nm. Consequently, a noticeable deviation from classical filtration theory might be present for particles below 20 nm. However, this phenomenon could be due to artifact particle counts of the CPC as aforementioned. Besides, Balazy et al. (2004) did not exclude electrostatic effects, since the particles were not neutralized, which might be a source of additional artifacts (Heim et al., 2005).

4. Conclusions

Penetrations of aerosol, size ranging from 4.5 nm to 10 μm, through fibrous filters were performed to explore the filtration characteristics of particles sized below 10 nm in diameter and to check previous experimental data (Balazy et al., 2004). Particle size was measured using an SMPS system equipped with a nano- or long-DMA and an APS. The results obtained can be summarized as follows:

1. The thermal rebound effect on nanoparticle collection was not observed in this work. Previous experimental studies reached erroneous conclusions because of unreliable particle number concentration measurements.
2. The respirators tested in this study are heavily reliant on their electrostatic charge to provide sufficient filtration efficiencies. The aerosol penetration values in the 10 nm–5 μm size range increased markedly with reducing electrostatic charge on the fibers of each filter and the most penetrating particle size shifted markedly from the nanometer-sized to submicrometer-sized range.

3. Almost all particles sized below 10 nm and above 5 μm were collected in the tested respirator filters, and the penetration values were not affected by the amount of filter charge. Consequently, diffusion is the only important mechanism for collection of particles less than 10 nm, and impaction and interception are the dominant mechanisms for collecting micrometer-sized particles.

References

Balazy, A., Podgorsky, A., & Gradon, L. (2004). Filtration of nanosized aerosol particles in fibrous filters I—experimental results. *Journal of Aerosol Science*, S967–S968. EAC Proceedings II.

Balazy, A., Toivola, M., Adhikari, A., Sivasubramani, S. K., Reponen, T., & Grinshpun, S. A. (2006a). Do N95 respirators provide 95% protection level against airborne viruses, and how adequate are surgical masks?. *American Journal of Infection Control*, *34*(2), 51–57.

Balazy, A., Toivola, M., Reponen, T., Podgórski, A., Zimmer, A., & Grinshpun, S. A. (2006b). Manikin-based performance evaluation of N95 filtering-facepiece respirators challenged with nanoparticles. *Annals of Occupational Hygiene*, *50*(3), 259–269.

Chen, C. C., & Huang, S. H. (1998). The effect of particle charge on the performance of an electret filtering facepiece. *American Industrial Hygiene Association Journal*, *59*, 227–233.

Chen, C. C., & Willeke, K. (1992). Characteristics of face seal leakage in filtering facepieces. *American Industrial Hygiene Association Journal*, *53*, 533–539.

Chen, C. C., Lehtimaki, M., & Willeke, K. (1992). Aerosol penetration through filtering facepieces and respirator cartridges. *American Industrial Hygiene Association Journal*, *53*, 566–574.

Chen, C. C., Lehtimaki, M., & Willeke, K. (1993). Loading and filtration characteristics of filtering facepieces. *American Industrial Hygiene Association Journal*, *54*(2), 51–60.

Dockery, D. W., & Pope, A. C. (1994). Acute respiratory effects of particulate air pollution. Annual Review of Public Health, 15, 107–132.

Donaldson, K., Li, X. Y., & Mac-Nee, W. (1998). Ultrafine (nanometre) particle mediated lung injury. Journal of Aerosol Science, 29, 553–560.

Hagdnagy, W., Stiller-Winkler, R., Kainka, R., Ranft, U., & Idel, H. (1998). Influence of urban air pollution on the immune system of children. Journal of Aerosol Science, Supplement 2, S997–S998.

Heim, M., Mullins, B., Wild, M., Meyer, J., & Kasper, G. (2005). Filtration efficiency of aerosol particles below 20 nm. *Aerosol Science and Technology*, *39*, 782–789.

Hinds, W. C. (1999). *Aerosol technology: Properties, behavior, and measurement of airborne particles*. (2nd ed), New York: Wiley, (pp. 182–205).

Kanaoka, C., Emi, H., Otani, Y., & Iiyama, T. (1987). Effect of charging state of particles on electret filtration. *Aerosol Science and Technology*, *7*, 1–13.

Lathrache, R., & Fissan, H. J. (1987). Enhancement of particle deposition in filters due to electrostatic effects. *Filtration & Separation*, *24*(6), 418–422.

Lee, K. W., & Liu, B. Y. H. (1982). Theoretical study of aerosol filtration by fibrous filter. *Aerosol Science and Technology*, *1*, 147–161.

Martin, S. B., & Moyer, E. S. (2000). Electrostatic respirator filter media: Filter efficiency and most penetrating particle size effects. *Applied Occupational & Environmental Hygiene*, *15*, 609–617.

McCullough, N. V., Brosseau, L. M., & Vesley, D. (1997). Collection of three bacterial aerosols by respirator and surgical mask filters under varying conditions of flow and relative humidity. *Annals of Occupational Hygiene*, *41*, 677–690.

Oberdorster, G., Ferin, J., Gelein, R., Soderholm, S. C., & Finkelstein, J. (1992). Role of the alveolar macrophage in lung injury: Studies with ultrafine particles. Environmental Health Perspectives, 97, 193–199.

Qian, Y., Willeke, K., Grinshpun, S. A., Donnelly, J., & Coffey, C. C. (1998). Performance of N95 respirators: Filtration efficiency for airborne microbial and inert particles. *American Industrial Hygiene Association Journal*, *59*, 128–132.

Tennal, K. B., Mazumder, M. K., Siag, A., & Reddy, R. N. (1991). Effect of loading with an oil aerosol on the collection efficiency of an electret filter. *Particulate Science and Technology*, *9*, 19–29.

TSI Inc. (2002). *Model 3934 scanning mobility particle sizer*: *Instruction manual*. USA: TSI Inc.

Wang, H. C., & Kasper, G. (1991). Filtration efficiency of nanometer-size aerosol particles. *Journal of Aerosol Science*, *22*, 31–41.

Willeke, K., Qian, Y., Donnelly, J., Grinshpun, S., & Ulevicius, V. (1996). Penetration of airborne microorganisms through a surgical mask and a dust/mist respirator. *American Industrial Hygiene Association Journal*, *57*, 348–355.

Further reading

Huang, C., Willeke, K., Qian, Y., Grinshpun, S., & Ulevicius, V. (1998). Method for measuring the spatial variability of aerosol penetration through respirator filters. *American Industrial Hygiene Association Journal*, *59*, 461–465.

Wang, C. S. (2001). Electrostatic forces in fibrous filters—a review. *Powder Technology*, *118*, 166–170.